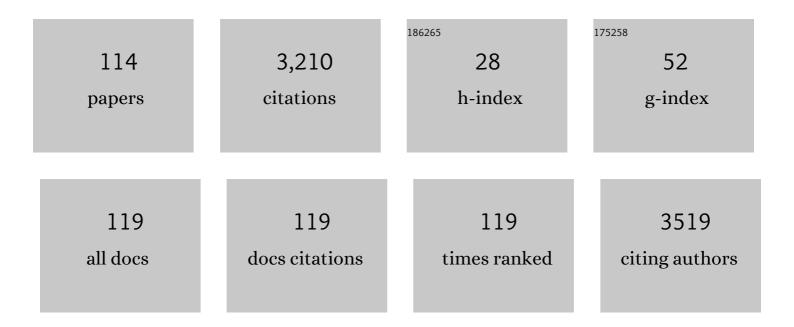
List of Publications by Year in descending order

Source: https://exaly.com/author-pdf/2213250/publications.pdf Version: 2024-02-01



#	Article	IF	CITATIONS
1	Nucleation mechanisms in a SiO2-Li2O-P2O5-ZrO2 biomedical glass-ceramic: Insights on crystallisation, residual glasses and Zr4+ structural environment. Journal of the European Ceramic Society, 2022, 42, 1762-1775.	5.7	16
2	In situ combined stress―and temperatureâ€dependent Raman spectroscopy of Liâ€doped (Na,K)NbO ₃ . Journal of the American Ceramic Society, 2022, 105, 2735-2743.	3.8	8
3	Glass formation, physical and structural investigation studies of the (90-x) Sb2O3-10WO3-xNaPO3 glasses. Materials Today Communications, 2022, 30, 103226.	1.9	0
4	Ultra-Short-Pulse Laser Filaments for Float Glass Cutting: Influence of Laser Parameters on Micro Cracks Formation. Frontiers in Physics, 2022, 10, .	2.1	4
5	Eu3+-doped lithium tellurite glasses prepared under vacuum condition: Spectroscopic investigation and energy transfer mechanism. Journal of Luminescence, 2022, 246, 118812.	3.1	3
6	Room temperature deposition of freestanding BaTiO3 films: temperature-induced irreversible structural and chemical relaxation. Journal of Materials Science, 2022, 57, 13264-13286.	3.7	2
7	Melting Curves of Triolein Polymorphs. JAOCS, Journal of the American Oil Chemists' Society, 2021, 98, 211-219.	1.9	0
8	Thermal Evolutions to Glass-Ceramics Bearing Calcium Tungstate Crystals in Borate Glasses Doped with Photoluminescent Eu3+ Ions. Materials, 2021, 14, 952.	2.9	7
9	Utilizing Rare-Earth-Elements Luminescence and Vibrational-Spectroscopies to Follow High Pressure Densification of Soda–Lime Glass. Materials, 2021, 14, 1831.	2.9	2
10	Impact of magnesium on the structure of aluminoborosilicate glasses: A solidâ€state NMR and Raman spectroscopy study. Journal of the American Ceramic Society, 2021, 104, 4518-4536.	3.8	26
11	Enhanced Electromechanical Response and Thermal Stability of 0.93(Na _{1/2} Bi _{1/2})TiO ₃ â€0.07BaTiO ₃ Through Aerosol Deposition of Base Metal Electrodes. Advanced Materials Interfaces, 2021, 8, 2100309.	3.7	7
12	Coupling Raman, Brillouin and Nd3+ Photo Luminescence Spectroscopy to Distinguish the Effect of Uniaxial Stress from Cooling Rate on Soda–Lime Silicate Glass. Materials, 2021, 14, 3584.	2.9	4
13	Cerium speciation in silicate glasses: Structure-property relationships. Journal of Non-Crystalline Solids, 2021, 563, 120785.	3.1	13
14	Correlation between mechanical and structural properties as a function of temperature within the TeO2–TiO2–ZnO ternary system. Journal of Non-Crystalline Solids, 2020, 528, 119716.	3.1	5
15	Development of magnesiumâ€aluminumâ€silicate glassâ€ceramics nucleated with Nb 2 O 5. International Journal of Applied Glass Science, 2020, 11, 155-169.	2.0	9
16	Determining the local pressure during aerosol deposition using glass memory. Journal of the American Ceramic Society, 2020, 103, 2443-2452.	3.8	11
17	Shape-anisotropic cobalt-germanium-borate glass flakes as novel Li-ion battery anodes. Powder Technology, 2020, 363, 218-231.	4.2	14
18	Cooling rate calibration and mapping of ultra-short pulsed laser modifications in fused silica by Raman and Brillouin spectroscopy. International Journal of Extreme Manufacturing, 2020, 2, 035001.	12.7	16

#	Article	IF	CITATIONS
19	Influence of Al2O3 Addition on Structure and Mechanical Properties of Borosilicate Glasses. Frontiers in Materials, 2020, 7, .	2.4	14
20	Surface Probing of Ultraâ€6hortâ€Pulse Laser Filament Cut Window Glass and the Impact on the Separation Behavior. Advanced Engineering Materials, 2020, 22, 2000471.	3.5	4
21	Relaxation behavior of densified sodium aluminoborate glass. Acta Materialia, 2020, 198, 153-167.	7.9	5
22	Strain-activated light-induced halide segregation in mixed-halide perovskite solids. Nature Communications, 2020, 11, 6328.	12.8	86
23	Modeling the effect of the addition of alumina on structural characteristics and tensile deformation response of aluminosilicate glasses. Ceramics International, 2020, 46, 21657-21666.	4.8	3
24	Low-temperature degradation increases the cyclic fatigue resistance of 3Y-TZP in bending. Dental Materials, 2020, 36, 1086-1095.	3.5	15
25	Effects of Medium pH and Preconditioning Treatment on Protein Adsorption on 45S5 Bioactive Glass Surfaces. Advanced Materials Interfaces, 2020, 7, 2000420.	3.7	12
26	Tailoring the Mechanical Properties of Metaluminous Aluminosilicate Glasses by Phosphate Incorporation. Frontiers in Materials, 2020, 7, .	2.4	11
27	The influence of codoping on optical properties and glass connectivity of silica fiber preforms. Ceramics International, 2020, 46, 26251-26259.	4.8	5
28	Influence of Vanadium on Optical and Mechanical Properties of Aluminosilicate Glasses. Frontiers in Materials, 2020, 7, .	2.4	17
29	Thermal and optical properties of binary magnesium tellurite glasses and their link to the glass structure. Journal of Alloys and Compounds, 2020, 823, 153781.	5.5	24
30	Spectroscopic study of the role of alkaline earth oxides in mixed borate glasses - site basicity, polarizability and glass structure. Journal of Non-Crystalline Solids, 2020, 533, 119892.	3.1	27
31	Indentation densification of fused silica assessed by raman spectroscopy and constitutive finite element analysis. Journal of the American Ceramic Society, 2020, 103, 3076-3088.	3.8	27
32	Structure—longitudinal sound velocity relationships in glassy anorthite (CaAl2Si2O8) up to 20 GPa: An in situ Raman and Brillouin spectroscopy study. Geochimica Et Cosmochimica Acta, 2019, 261, 132-144.	3.9	9
33	Wet-chemical porosification of LTCC substrates: Dissolution mechanism and mechanical properties. Microporous and Mesoporous Materials, 2019, 288, 109593.	4.4	7
34	Evidence of polyamorphic transitions during densified SiO2 glass annealing. Journal of Chemical Physics, 2019, 151, 164502.	3.0	14
35	Bioactive glass coating using aerosol deposition. Ceramics International, 2019, 45, 14728-14732.	4.8	10
36	Structural and optical characterization of crystals obtained via solid state reactions in the In2O3–TiO2–Al2O3 pseudoternary system. SN Applied Sciences, 2019, 1, 1.	2.9	1

3

#	Article	IF	CITATIONS
37	Europium-Doped Tellurite Glasses: The Eu2+ Emission in Tellurite, Adjusting Eu2+ and Eu3+ Emissions toward White Light Emission. Materials, 2019, 12, 4140.	2.9	22
38	Colors in Glasses. Springer Handbooks, 2019, , 297-342.	0.6	11
39	Glass Machining and In-situ Metrology: recovery of spatio-temporal phase distribution from 2-dimensional interference fringe movement caused by irradiation of glass with ultra-short laser pulses at high pulse repetition rates. , 2019, , .		О
40	Fluorescence line narrowing and Judd-Ofelt theory analyses of <mml:math xmlns:mml="http://www.w3.org/1998/Math/MathML" altimg="si0042.gif" overflow="scroll"><mml:msup><mml:mrow><mml:mi>Eu</mml:mi></mml:mrow><mml:mrow><mml:mn>3low-silica calcium aluminosilicate glass and glass-ceramic. Journal of Luminescence, 2018, 201, 123-128.</mml:mn></mml:mrow></mml:msup></mml:math 	nml:mh> <r< td=""><td>nml:mo>+</td></r<>	nml:mo>+
41	Fracture anisotropy in texturized lithium disilicate glass-ceramics. Journal of Non-Crystalline Solids, 2018, 481, 457-469.	3.1	39
42	Development and characterization of niobium-releasing silicate bioactive glasses for tissue engineering applications. Journal of the European Ceramic Society, 2018, 38, 871-876.	5.7	33
43	Combined Differential scanning calorimetry, Raman and Brillouin spectroscopies: A multiscale approach for materials investigation. Analytica Chimica Acta, 2018, 998, 37-44.	5.4	26
44	Effect of thermally induced structural disorder on the chemical durability of International Simple Glass. Npj Materials Degradation, 2018, 2, .	5.8	37
45	Analysis of shockwave formation in glass welding by ultra-short pulses. Procedia CIRP, 2018, 74, 339-343.	1.9	3
46	Devitrification Behavior of Sol-Gel Derived ZrO2-SiO2 Rare-Earth Doped Glasses: Correlation between Structural and Optical Properties. Ceramics, 2018, 1, 274-286.	2.6	6
47	Optical Properties and Bismuth Redox in Bi-Doped High-Silica Al–Si Glasses. Journal of Physical Chemistry C, 2018, 122, 19777-19792.	3.1	19
48	Luminescent properties of Eu-doped calcium aluminosilicate glass-ceramics: A potential tunable luminophore. Optical Materials, 2018, 85, 41-47.	3.6	13
49	Chairside CAD/CAM materials. Part 1: Measurement of elastic constants and microstructural characterization. Dental Materials, 2017, 33, 84-98.	3.5	287
50	Relaxation processes of densified silica glass. Journal of Chemical Physics, 2017, 146, .	3.0	30
51	Decoupling of viscosity and relaxation processes in supercooled water: a molecular dynamics study with the TIP4P/2005f model. Physical Chemistry Chemical Physics, 2017, 19, 2124-2130.	2.8	37
52	Assessment of elastic models in supercooled water: A molecular dynamics study with the TIP4P/2005f force field. Journal of Chemical Physics, 2017, 147, 014504.	3.0	10
53	Cerium/aluminum correlation in aluminosilicate glasses and optical silica fiber preforms. Journal of Non-Crystalline Solids, 2017, 475, 85-95.	3.1	24
54	Chemical tunability of europium emission in phosphate glasses. Journal of Luminescence, 2017, 183, 53-61.	3.1	20

#	Article	IF	CITATIONS
55	On the induction of homogeneous bulk crystallization in Eu-doped calcium aluminosilicate glass by applying simultaneous high pressure and temperature. Journal of Applied Physics, 2016, 119, 245901.	2.5	3
56	Ca neighbors from XANES spectroscopy: A tool to investigate structure, redox, and nucleation processes in silicate glasses, melts, and crystals. American Mineralogist, 2016, 101, 1232-1235.	1.9	18
57	<i>In situ</i> structural analysis of calcium aluminosilicate glasses under high pressure. Journal of Physics Condensed Matter, 2016, 28, 315402.	1.8	15
58	Synthesis and luminescent properties of Eu3+/Eu2+ co-doped calcium aluminosilicate glass–ceramics. Journal of Luminescence, 2016, 169, 528-533.	3.1	29
59	The structure of haplobasaltic glasses investigated using X-ray absorption near edge structure (XANES) spectroscopy at the Si, Al, Mg, and O K -edges and Ca, Si, and Al L 2,3 -edges. Chemical Geology, 2016, 420, 213-230.	3.3	18
60	In situ structural changes of amorphous diopside (CaMgSi2O6) up to 20 GPa: A Raman and O K-edge X-ray Raman spectroscopic study. Geochimica Et Cosmochimica Acta, 2016, 178, 41-61.	3.9	26
61	Development and characterization of lithium-releasing silicate bioactive glasses and their scaffolds for bone repair. Journal of Non-Crystalline Solids, 2016, 432, 65-72.	3.1	63
62	Local densification of a single micron sized silica sphere by uniaxial compression. Scripta Materialia, 2015, 108, 84-87.	5.2	28
63	Emission tunability and local environment in europium-doped OHâ^'-free calcium aluminosilicate glasses for artificial lighting applications. Materials Chemistry and Physics, 2015, 156, 214-219.	4.0	25
64	19. In situ High-Temperature Experiments. , 2014, , 779-802.		0
65	13. Advances in Raman Spectroscopy Applied to Earth and Material Sciences. , 2014, , 509-542.		2
66	Pressure-independent Brillouin Fiber Optic Sensors for temperature measurements. Journal of Non-Crystalline Solids, 2014, 401, 36-39.	3.1	5
67	Phase Transformation in Laserâ€Induced Microâ€Explosion in Olivine (Fe,Mg) ₂ SiO ₄ . Advanced Engineering Materials, 2014, 16, 767-773.	3.5	16
68	Advances in Raman Spectroscopy Applied to Earth and Material Sciences. Reviews in Mineralogy and Geochemistry, 2014, 78, 509-541.	4.8	135
69	Irradiated rareâ€earthâ€doped powellite single crystal probed by confocal Raman mapping and transmission electron microscopy. Journal of Raman Spectroscopy, 2014, 45, 383-391.	2.5	15
70	Progress and challenges in advanced ground-based gravitational-wave detectors. General Relativity and Gravitation, 2014, 46, 1.	2.0	2
71	In situ High-Temperature Experiments. Reviews in Mineralogy and Geochemistry, 2014, 78, 779-800.	4.8	27
72	Polyamorphic transitions in silica glass. Journal of Non-Crystalline Solids, 2013, 382, 133-136.	3.1	32

#	Article	IF	CITATIONS
73	Photoreduction of iron by a synchrotron X-ray beam in low iron content soda-lime silicate glasses. Chemical Geology, 2013, 346, 106-112.	3.3	26
74	Raman Spectroscopy of Adsorbed Water in Clays: First Attempt at Band Assignment. Procedia Earth and Planetary Science, 2013, 7, 203-206.	0.6	13
75	Mapping of rare earth elements in nuclear waste glass–ceramic using micro laser-induced breakdown spectroscopy. Spectrochimica Acta, Part B: Atomic Spectroscopy, 2013, 87, 139-146.	2.9	55
76	Dynamics of iron-bearing borosilicate melts: Effects of melt structure and composition on viscosity, electrical conductivity and kinetics of redox reactions. Journal of Non-Crystalline Solids, 2013, 373-374, 18-27.	3.1	15
77	Permanent densification of compressed silica glass: a Raman-density calibration curve. Journal of Physics Condensed Matter, 2013, 25, 025402.	1.8	70
78	Chemical Durability of Lanthanumâ€Enriched Borosilicate Glass. International Journal of Applied Glass Science, 2013, 4, 383-394.	2.0	23
79	<i>In situ</i> Brillouin study of sodium alumino silicate glasses under pressure. Journal of Chemical Physics, 2013, 139, 074501.	3.0	26
80	Experimental study of dissolution rates of hedenbergitic clinopyroxene at high temperatures: dissolution in water from 25 °C to 374 °C. European Journal of Mineralogy, 2013, 25, 353-372.	1.3	16
81	Low-frequency Raman scattering under high pressure in diamond anvil cell: Experimental protocol and application to GeO2 and SiO2 boson peaks. Journal of Non-Crystalline Solids, 2012, 358, 3156-3160.	3.1	10
82	Progressive transformations of silica glass upon densification. Journal of Chemical Physics, 2012, 137, 124505.	3.0	51
83	Effect of temperature and thermal history on borosilicate glass structure. Physical Review B, 2012, 85,	3.2	117
84	Correlation between boson peak and anomalous elastic behavior in GeO2 glass: An <i>in situ</i> Raman scattering study under high-pressure. Journal of Chemical Physics, 2011, 134, 234503.	3.0	24
85	Femtosecond laser induced density changes in GeO_2 and SiO_2 glasses: fictive temperature effect [Invited]. Optical Materials Express, 2011, 1, 605.	3.0	53
86	Observation of O_2 inside voids formed in GeO_2 glass by tightly-focused fs-laser pulses. Optical Materials Express, 2011, 1, 1150.	3.0	39
87	Laser-induced structural changes in pure GeO2 glasses. Journal of Non-Crystalline Solids, 2011, 357, 2637-2640.	3.1	10
88	Behaviour of the Eu3+ 5D0→7F0 transition in CaMoO4 powellite type ceramics under Ar and Pb ions implantation. Optical Materials, 2011, 34, 386-390.	3.6	21
89	Structural heterogeneity and pressure-relaxation in compressed borosilicate glasses by in situ small angle X-ray scattering. Journal of Chemical Physics, 2011, 134, 204502.	3.0	32
90	Luminescent centres in pezzottaite, CsBe2LiAl2Si6O18. European Journal of Mineralogy, 2010, 22, 605-612.	1.3	7

#	Article	IF	CITATIONS
91	Boron Speciation in Sodaâ€Lime Borosilicate Glasses Containing Zirconium. Journal of the American Ceramic Society, 2010, 93, 2693-2704.	3.8	111
92	Permanent Ge Coordination Change Induced by Pressure in La ₂ O ₃ –B ₂ O ₃ –GeO ₂ Glass. Journal of the American Ceramic Society, 2010, 93, 2726-2730.	3.8	2
93	Effect of chemical composition on borosilicate glass behavior under irradiation. Journal of Non-Crystalline Solids, 2010, 356, 388-393.	3.1	117
94	The crystal and melt structure of spinel and alumina at high temperature: An in-situ XANES study at the Al and Mg K-edge. Geochimica Et Cosmochimica Acta, 2009, 73, 3410-3422.	3.9	45
95	Silica polymorphs, glass and melt: An in situ high temperature XAS study at the Si K-edge. Journal of Non-Crystalline Solids, 2009, 355, 1099-1102.	3.1	25
96	Elastic anomalous behavior of silica glass under high-pressure: In-situ Raman study. Journal of Non-Crystalline Solids, 2009, 355, 1095-1098.	3.1	38
97	Silica under hydrostatic pressure: A non continuous medium behavior. Journal of Non-Crystalline Solids, 2009, 355, 2422-2424.	3.1	34
98	Structure of spinel at high temperature using <i>in-situ</i> XANES study at the Al and Mg K-edge. Journal of Physics: Conference Series, 2009, 190, 012178.	0.4	2
99	Kinetics of iron redox reaction in silicate melts: A high temperature Xanes study on an alkali basalt. Journal of Physics: Conference Series, 2009, 190, 012182.	0.4	10
100	Contribution of neodymium optical spectroscopy to the crystal growth study of a silicate apatite in a glassy matrix. Optical Materials, 2008, 30, 1694-1698.	3.6	8
101	Simulation of Eu3+ luminescence spectra of borosilicate glasses by molecular dynamics calculations. Optical Materials, 2008, 30, 1689-1693.	3.6	5
102	Environments around Al, Si, and Ca in aluminate and aluminosilicate melts by X-ray absorption spectroscopy at high temperature. American Mineralogist, 2008, 93, 228-234.	1.9	86
103	Kinetics and mechanisms of iron redox reactions in silicate melts: The effects of temperature and alkali cations. Geochimica Et Cosmochimica Acta, 2008, 72, 2157-2168.	3.9	105
104	Iron Redox Reactions in Model Nuclear Waste Glasses and Melts. Materials Research Society Symposia Proceedings, 2008, 1124, 1.	0.1	2
105	The Silicon Environment in Silica Polymorphs, Aluminosilicate Crystals and Melts: An In Situ High Temperature XAS Study. AIP Conference Proceedings, 2007, , .	0.4	0
106	Investigation of Aluminate and Al2O3 Crystals and Melts at High Temperature Using XANES Spectroscopy. AlP Conference Proceedings, 2007, , .	0.4	3
107	An In Situ High Temperature Investigation of Cation Environments in Aluminate and Silicate Glasses and Liquids at the LUCIA Beamline. AIP Conference Proceedings, 2007, , .	0.4	1
108	Behaviour of simplified nuclear waste glasses under gold ions implantation: A microluminescence study. Journal of Nuclear Materials, 2007, 362, 480-484.	2.7	15

#	Article	IF	CITATIONS
109	Low-temperature heat capacity of GeO2 and B2O3 glasses: thermophysical and structural implications. Journal of Non-Crystalline Solids, 2003, 315, 20-30.	3.1	32
110	Heat capacity and entropy of rutile (TiO 2) and nepheline (NaAlSiO 4). Physics and Chemistry of Minerals, 2002, 29, 267-272.	0.8	40
111	Energetics of kaolin polymorphs. American Mineralogist, 1999, 84, 506-516.	1.9	43
112	Entropy of calcium and magnesium aluminosilicate glasses. Chemical Geology, 1996, 128, 113-128.	3.3	24
113	High-temperature heat capacity and thermal expansion ofSrTiO3andSrZrO3perovskites. Physical Review B, 1996, 53, 3013-3022.	3.2	301
114	Raman and fluorescence. , 0, , 61-82.		9